RESEARCH/REVIEW ARTICLE

Late winter biogeochemical conditions under sea ice in the Canadian High Arctic

Helen S. Findlay,[1] Laura A. Edwards,[2,3] Ceri N. Lewis,[4] Glenn A. Cooper,[5] Robert Clement,[6] Nick Hardman-Mountford,[7] Svein Vagle[5] & Lisa A. Miller[5]

[1] Plymouth Marine Laboratory, Prospect Place, West Hoe, Plymouth PL1 3DH, UK
[2] Centre for Applied Marine Sciences, Menai Science Laboratories, Bangor University, Menai Bridge, Anglesey LL59 5AB, UK
[3] Geography, School of Environment, Education and Development, University of Manchester, Oxford Road, Manchester M13 9PL, UK
[4] College of Life and Environmental Sciences, University of Exeter, Hatherly Laboratories, Prince of Wales Road, Exeter EX4 4PS, UK
[5] Institute of Ocean Sciences, Fisheries and Oceans Canada, Sidney, British Columbia V8L 4B2, Canada
[6] School of Geoscience, University of Edinburgh, 202 Crew Building, Edinburgh EH9 3JN, Scotland, UK
[7] The Commonwealth Scientific and Industrial Research Organisation, Marine and Atmospheric Research, Underwood Avenue, Floreat WA 6014, Australia

Keywords
Sea ice; carbon cycling; biogeochemical cycles; nutrients; Arctic Ocean; ocean acidification.

Correspondence
Helen S. Findlay, Plymouth Marine Laboratory, Prospect Place, West Hoe, Plymouth PL1 3DH, UK.
E-mail: hefi@pml.ac.uk

Abstract

With the Arctic summer sea-ice extent in decline, questions are arising as to how changes in sea-ice dynamics might affect biogeochemical cycling and phenomena such as carbon dioxide (CO_2) uptake and ocean acidification. Recent field research in these areas has concentrated on biogeochemical and CO_2 measurements during spring, summer or autumn, but there are few data for the winter or winter–spring transition, particularly in the High Arctic. Here, we present carbon and nutrient data within and under sea ice measured during the Catlin Arctic Survey, over 40 days in March and April 2010, off Ellef Ringnes Island (78° 43.11′ N, 104° 47.44′ W) in the Canadian High Arctic. Results show relatively low surface water (1–10 m) nitrate (<1.3 μM) and total inorganic carbon concentrations (mean $\pm$ SD $= 2015 \pm 5.83$ μmol kg^{-1}), total alkalinity (mean $\pm$ SD $= 2134 \pm 11.09$ μmol kg^{-1}) and under-ice pCO_{2sw} (mean $\pm$ SD $= 286 \pm 17$ μatm). These surprisingly low wintertime carbon and nutrient conditions suggest that the outer Canadian Arctic Archipelago region is nitrate-limited on account of sluggish mixing among the multi-year ice regions of the High Arctic, which could temper the potential of widespread under-ice and open-water phytoplankton blooms later in the season.

The Arctic Ocean has increasingly become the focus of climate change and ocean acidification research as better technology and the reduction in sea-ice extent (e.g., Perovich et al. 2008) allow improved access to the Arctic. One of the key questions is the impact of changes in sea ice on the biogeochemistry of the Arctic system. Although complex sea-ice processes are now being incorporated into global climate models (Orr et al. 2009; Popova et al. 2010), there is still much uncertainty about ice-associated processes and few available data to validate model predictions.

Field data have predominantly been collected in the Arctic Ocean during the late spring, summer and early autumn from ships or ice camps, but rarely in winter because of the difficult sampling conditions. Indeed, few data of inorganic carbon and nutrients exist for the late winter–early spring period in the Arctic (Bates & Mathis 2009; Miller et al. 2011; Shadwick et al. 2011; Brown et al. 2015), and virtually no data are available for the northern edge of the Canadian Arctic Archipelago (Stein & Macdonald 2004; Bates & Mathis 2009). In more temperate seasonally driven systems, the winter period is when surface ocean conditions are "reset." For example, in the sub-Arctic Norwegian and Icelandic seas, winter mixing processes, together with changes in temperature and

Citation: *Polar Research* 2015, *34*, 24170, http://dx.doi.org/10.3402/polar.v34.24170

salinity, allow new nutrients to be introduced into the surface waters (Findlay et al. 2008; Skjelvan et al. 2008; Olafsson et al. 2009; Shadwick et al. 2013). Winter mixing, combined with low productivity levels, also have consequences for the carbon concentration in surface waters. Subsurface water containing higher CO_2 concentrations can be entrained upwards in well-mixed systems (e.g., Miller et al. 1999). In addition, the principally heterotrophic systems in the surface ocean over winter will act to increase the CO_2 concentration (Findlay et al. 2008; Bates et al. 2009; Olafsson et al. 2009). Ultimately, the conditions at the end of winter will influence the timing, extent and magnitude of primary production (and other biological processes) in spring (e.g., Popova et al. 2010) and consequently will influence the carbon and carbonate cycles.

In the Canadian High Arctic, the dynamics are somewhat different: offshore, in the deep Canada Basin, the shallow surface mixed layer rarely deepens beyond about 25 m, is deepest in winter and shoals to about 16 m in summer (Toole et al. 2010). Wind stress is a significant driver of mixing, acting either directly on the mixed layer or on the overlying ice floes, which produce surface currents. Shear mixing between the surface and underlying layers also can contribute to convection (Krishfield et al. 2008). However in the central Canada Basin, the strong density stratification at the base of the mixed layer, as well as efficient lateral mixed layer restratification processes, inhibits surface layer deepening, thereby limiting fluxes to the surface (Toole et al. 2010). In shallower regions of the Canadian Arctic Archipelago and surrounding seas, tidal dynamics also play an important role in mixing, although ice cover dampens the tidal amplitude as well dampening the effects of storm-generated mixing (Prinsenberg & Ingram 1991). Additionally, density variations due to ice formation and melt can cause internal mixing, with salt rejection from ice growth during winter leading to a deepening of the mixed layer, for example, the central Hudson Bay mixed layer deepens to >100 m (Prinsenberg & Ingram 1991). Many coastal regions are stratified by freshwater run-off, resulting in thinner winter mixed layers and reduced vertical exchange, but observations within the Canadian Arctic Archipelago showed that the surface mixed layer varied little over a seasonal cycle because of limited input from river waters (Prinsenberg & Ingram 1991). As our study site was remote from rivers, we might expect the waters we sampled to be well mixed; the exposure of our location to the pack ice of the central Arctic could also foster strong stratification from seasonal ice-melt, as is typical of the Canada Basin.

Understanding the conditions under ice cover at the end of winter, as light levels increase, at the boundary between the Canadian Arctic Archipelago and the offshore Canada Basin is crucial to understanding the seasonal biogeochemical cycling dynamics of the High Arctic and to informing predictive models. Indeed, models currently show large discrepancies when they attempt to capture the seasonal dynamics of carbonate in the Arctic Ocean (Orr et al. 2010; Popova et al. 2014).

Here, we present nutrient and carbon data within and under Arctic sea ice, alongside associated biological and physical conditions during the late winter and early spring of 2010. We aim to assess the late winter conditions with respect to physical mixing and the onset of primary production, and how these factors can result in a drawdown of carbon and nutrients within the surface layer. In March and April 2010, we participated in the Catlin Arctic Survey (CAS) and were stationed at an ice base located at 78° 43.11′ N, 104° 47.44′ W, off Ellef Ringnes Island in the Canadian Arctic Archipelago (Fig. 1a). The ice base was attached to land-fast ice, so there was no spatial movement during the field season. The ice base was located on the Canadian continental shelf (at a water depth greater than 250 m) and, therefore, the surface waters at the camp could be exposed to currents that circulate from the Pacific Ocean along the edge of the Canada Basin and enter the archipelago (Jones et al. 1998; Nguyen et al. 2011). The offshore Arctic Ocean, around the northern edge of Ellesmere Island and Greenland, can remain ice-covered year round as a result of the build-up of multi-year ice (Flato & Brown 1996; Comiso 2003).

Materials and methods

Ice base

From 15 March 2010 to 30 April 2010, the Catlin Ice Base (CIB) was situated on a region of flat, first-year sea ice, which extended east to west from Ellef Ringnes Island seaward (Fig. 1a, c). The thickness of the sea ice in the area was between 1.5 and 1.7 m. The science sampling site was located 2 km west of the CIB at 78° 42.69′ N, 104° 52.66′ W. An ice hole, 1.3 x 1.1 m in size, was made on 16 March 2010. The ice thickness at the hole was 1.52 m, with 0.2 m freeboard. The hole was covered with a Polar Chief tent to minimize freezing during sampling. The water depth under the ice was not precisely known, although the maximum depth of the wire on the winch used for obtaining samples was roughly 230 m. The Canadian Hydrographic Service Chart #7953 (last updated 17 March 1972) suggests that the area is between soundings of 290 and 420 m.

Citation: *Polar Research* 2015, *34*, 24170, http://dx.doi.org/10.3402/polar.v34.24170

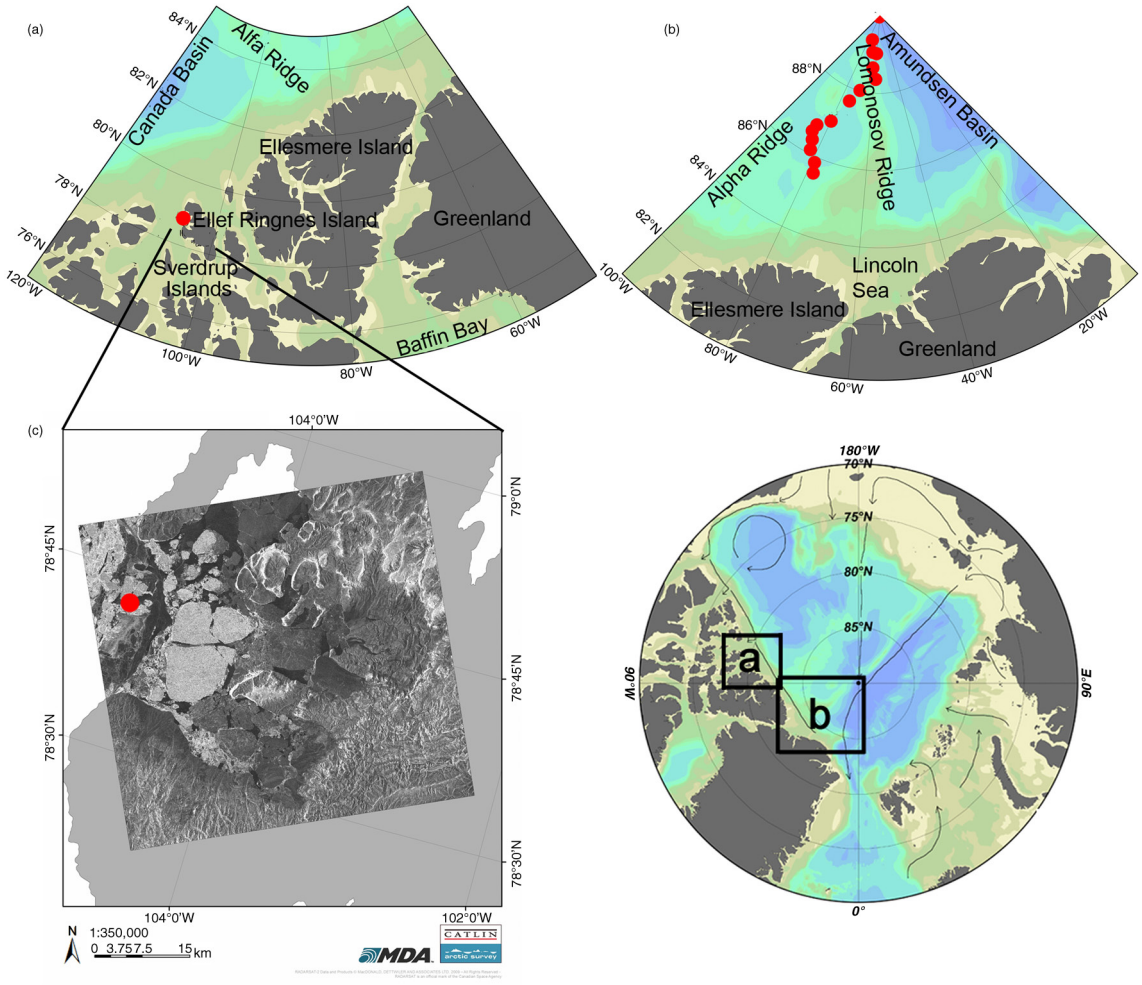

Fig. 1 Bathymetric maps showing the Arctic Ocean. The Catlin Arctic Survey ice base (CIB) is marked with a red dot (78°N, 104°W) on map (a). The Catlin Arctic Survey expedition transect sampling locations are marked with red dots on map (b) between 85°N to 90°N. (c) An enlarged map of Deer Bay overlaid with a satellite image from 8 February 2010, also showing the location of the CIB marked by a red dot.

CIB meteorological measurements

A model 7425 Weather Wizard III meteorological station (Davis Instruments, Hayward, CA, USA) was set up at the CIB to measure wind speed, wind direction (from an anemometer placed 3 m above the sea ice) and shaded air temperature. These parameters were recorded twice daily (at 09:00 and 21:00, local time), as well as observations of cloud cover (oktas) and general weather conditions.

CIB seawater sampling

Seawater sampling was carried out through the ice hole every four days, starting on 17 March 2010 (Day of Year [DoY] 75) and ending on 26 April 2010 (DoY 115). Conductivity, temperature and depth measurements were made on each sample day using an SBE 19plus SeaCAT conductivity–temperature–depth (CTD) instrument (Sea-Bird Electronics, Bellevue, WA, USA), calibrated using bottle salinity samples analysed on an Autosal 8400B salinometer (Guildline Instruments, Smiths Falls, ON, Canada) at the Institute of Ocean Sciences, Sidney, Canada. Seawater was collected for analysis on each sample day from 1-, 3-, 5- and 10-m depths under the sea ice, using a 5-L Niskin bottle. Additionally, samples were taken at 100 and 200 m on 21 and 22 April 2010.

CIB sea-ice sampling

Four ice cores were collected from within 50 m of the water sampling hole on 8 and 13 April 2010 (DoY 97 and 102, respectively) using a 9-cm internal diameter ice corer (Kovacs Enterprises, Roseburg, OR, USA). A 1-m^2 area

of ice was cleared of snow, and snow depth was measured at the edge of the cleared area. Once the cores were retrieved, ice thickness was measured using a tape measure with a weighted catch attachment deployed through the hole. The cores were immediately laid out on a cleaned PVC sled. Each core was then cut into sections using a clean stainless steel saw (starting from the top). Each piece was individually placed in a polyethylene, resealable, zip-seal bag and transported back to the CIB. Pieces from each of the "top," "middle" and "bottom" sections of the core (Table 1) were then placed into gas-tight Tedlar bags, and a hand-pump was used to remove the headspace. The bagged sections were left in the dark to melt at room temperature, which took approximately 24 h. Once the ice melted, water samples were collected from each bag using methods described in a subsequent section for total inorganic carbon (C_T), total alkalinity (A_T), salinity, oxygen-18 (δO^{18}), nutrients and chlorophyll. The cold, brittleness of the ice and logistics prevented any additional cores from being collected.

Spatial transect from 85°N to 90°N

Spatial data of nutrients, chlorophyll, C_T and A_T were additionally collected through sea ice by a second team travelling on foot from 85°N to the North Pole (Fig. 1b) from 15 March 2010 to 12 May 2010, hereafter referred to as the Catlin Explorer Transect (CET). Seawater was collected through ice holes drilled with a Mora 110-mm ice auger (Rapala, Vääksy, Finland) and using a 1.2-L Kemmerer bottle from 1 m and 10 m under the sea ice. Duplicate C_T/A_T samples were collected into boreo-silicate square bottles with screw-cap lids and fixed with 100 µl of saturated $HgCl_2$. These bottles were housed in specially designed warm boxes (adapted Yeti boxes) which had battery-operated heating mats placed in the bottoms to maintain the temperature above freezing. The samples were picked up from the expedition team and flown out on each resupply flight roughly every 18 days. Temperature and salinity profiles were made from the surface to approximately 30 m using an XR-420 CTD instrument (RBR, Kanata, ON, Canada) at each sampling location.

Table 1 Ice core collection data, size of each section (top, middle and bottom), total core length and snow cover.

	Ice core			
	1	2	3	4
Collection date	08/04/10	08/04/10	13/04/10	13/04/10
Top (cm)	0–54	0–56	0–62	0–52
Mid (cm)	54–118	56–112	62–121	52–104
Bottom (cm)	118–172	112–170	121–177	104–163
Total length (cm)	172	170	177	163
Snow cover (cm)	4.5	2	5	3

Sample processing and measurements

Chlorophyll. Seawater and ice-melts were filtered through grade GF/F filters (from the nutrient filtration), which were stored (frozen at −20°C) and returned to Plymouth Marine Laboratory, Plymouth, UK, for chlorophyll analysis. Each filter was placed in 90% v/v acetone and left for extraction at room temperature in the dark for 24 h. Concentrations of chlorophyll were measured using a model 10-AU fluorometer (Turner Designs, Sunnyvale, CA, USA) following US Joint Global Ocean Flux Study protocols (Knap et al. 1996).

Inorganic nutrients. Fifty millilitres of collected seawater and ice core meltwater were filtered (GF/F filters) into acid-cleaned, aged, 60-mL bottles (Nalgene, Rochester, NY, USA). Bottles were stored and shipped back frozen (−20°C) to land. Analysis was carried out at Plymouth Marine Laboratory (Woodward & Rees 2001) using a Bran & Luebbe AAIII segmented flow autoanalyser (SPX Flow Technology Norderstedt, Germany) for the colourimetric determination of inorganic nutrients: combined nitrate + nitrite (Brewer & Riley 1965), nitrite (Grasshoff 1976), phosphate (Zhang & Chi 2002), silicate (Kirkwood 1989) and ammonium (Mantoura & Woodward 1983). Nitrate concentrations were calculated by subtracting the nitrite from the combined nitrate + nitrite concentration.

Inorganic carbon. Seawater samples for total inorganic carbon (C_T) and total alkalinity (A_T) were collected in triplicate into 250-ml Duran glass bottles with ground glass stoppers for the 1-, 3-, 5- and 10-m samples according to Dickson et al. (2007). For the deep water samples (100 and 200 m) at the CIB wide-mouth, screw-cap glass bottles were used, while for the CET samples narrow-mouth, screw-cap bottles were used. For the melted ice cores, water was transferred from the Tedlar bags to 250-mL Duran glass bottles by attaching tubing to the valve inset in the bag and filling the bottles as recommended by Dickson et al. (2007). Samples were poisoned with 100 µL saturated $HgCl_2$, as recommended by Dickson et al. (2007). Samples were stored at 4°C to the extent possible (sample storage temperature was difficult to control at the camp) in the dark and analysed at the Institute of Ocean Sciences within one year of collection, using VINDTA (Marianda, Kiel, Germany) and SOMMA (Marianda) instrumentation for C_T and an open-cell potentiometric titration with non-linear least squares curve fitting for A_T (Dickson et al. 2007). Batch 101 CRM (provided by

Citation: *Polar Research* 2015, *34*, 24170, http://dx.doi.org/10.3402/polar.v34.24170

Andrew Dickson, Scripps Institute of Oceanography) was used for calibration. Precision across CIB measurements was 2.3 μmol kg^{-1} for C_T and 5.7 μmol kg^{-1} for A_T. There was a decrease in the precision of the C_T analysis (about 4 umol kg^{-1}) for the CIB deep samples preserved in the wide-mouth, screw-cap bottle, likely because these bottles had greater potential for gas exchange during sampling, transport and analysis. Precision across CET measurements was 16 μmol kg^{-1} for C_T and 20 μmol kg^{-1} for A_T. Assuming that the deep water (100 and 200 m) samples from the CIB were supersaturated and the CET samples were slightly undersaturated, any errors associated with the screw-cap bottles will lead to underestimates for the deep water samples at the CIB and possibly smaller overestimates for the CET samples.

The seawater carbonate system programme CO2SYS (Pierrot et al. 2006) was used to calculate the CO_2 partial pressure (pCO_2) and pH_T from C_T, A_T, in situ temperature, salinity and silicate and phosphate concentrations. Carbonic acid dissociation constants of Mehrbach et al. (1973) refit by Dickson & Millero (1987) and the HSO_4^- constant of Dickson (1990) were used. These calculations were not made for the ice core melt samples.

Stable oxygen isotopes. Samples for ^{18}O:^{16}O (reported as δO18) ratios from both water column and ice-melt samples were analysed by the G.G. Hatch Isotope Laboratories at the University of Ottawa, Ottawa, Canada, on a DeltaPlus XP isotope ratio mass spectrometer (Thermo Finnigan, San Jose, CA. USA) after headspace gas equilibration. The analytical precision was estimated to be 0.15 per mil.

Atmospheric CO_2 and flux measurements. An eddy covariance system (ECS) was used to measure atmospheric CO_2 and CO_2 fluxes between the ice and the atmosphere. The ECS consisted of a closed-path LI7000 infrared gas analyser (Li-Cor Biosciences, Lincoln, NE, USA), sample pump, purge column, battery and CR5000 logger/signal unit (Campbell Scientific, Logan, UT, USA) housed in an insulated box container. A sonic anemometer and gas inlet pipe, with an external heat exchanger for equilibration of incoming air, were located at the top of a 3-m mast next to the control unit box. The ECS was sited approximately 230 m north-west of the main ice base on flat ice (snow depth <5 cm) between rubble ice regions 290 m to the south and 700 m to the north. The extreme cold conditions during the first 20 days of the expedition caused some difficulties with the ECS. However, the ECS was run successfully between 25 and 29 April 2010. ECS data were processed using EdiRe analysis software following the standard Euroflux guidelines (Aubinet et al. 2000). Because of the limited data availability, natural coordinate rotations (Tanner & Thurtell 1969) were employed for anemometer velocity data. The turbulent tube attenuation of Massman (1991) was employed in the frequency response corrections (Moore 1986). Fluxes were calculated for half-hour intervals and averaged to daily values assuming stationarity of environmental conditions. Data from the Alert atmospheric monitoring station (82° 27′ N, 62° 30′ W) were obtained to assess the quality of our ECS atmospheric pCO_2 data and to obtain data for the period prior to 25 April 2010 (Dlugokencky et al. 2015).

Water column backscatter and current shear. A self-contained Workhorse Sentinel acoustic doppler current profiler (ADCP; Teledyne RD Instruments, Poway, CA, USA) was mounted on an aluminium bar, anchored to the top of the ice and deployed just below the bottom of the ice to monitor acoustical backscatter and tidal currents. The instrument was operated nearly continuously for three days at the end of March, at 307 kHz, with bin sizes of 4 m and with the first bin at 6.09 m below the ice. Each ensemble was separated by 66 s and consisted of 50 transmissions, or pings. Because of the low concentration of scatterers in the water column the effective range of the instrument was approximately 45 m.

Results

The results described in the first four sections below are for the CIB, which was occupied from 15 March 2010 to 30 April 2010 (DoY 73 to 119) and is the main focus of this study. The final results section provides details for the CET.

CIB physical conditions

Atmospheric conditions. From 17 March 2010 (DoY 75) to 9 April 2010 (DoY 98), air temperature was predominantly below −20°C, with dominant winds from the north and north-west. From the 10 to 27 April 2010 (DoY 99 to 116) air temperature began to vary more substantially on a daily basis and rarely dropped below −20°C, occasionally warming to as high as −3°C (Fig. 2). The dominant wind direction during this second phase was from the south and south-east. There was approximately 5 cm of snow covering the ice at the time of first sampling, but snowfall during the rest of the field season resulted in snow thickness increasing to between 10 and 15 cm towards late April.

Seawater conditions. Temperature and salinity both increased with depth (Fig. 3). The temperature in the top 25 m of the water column was well mixed and with a

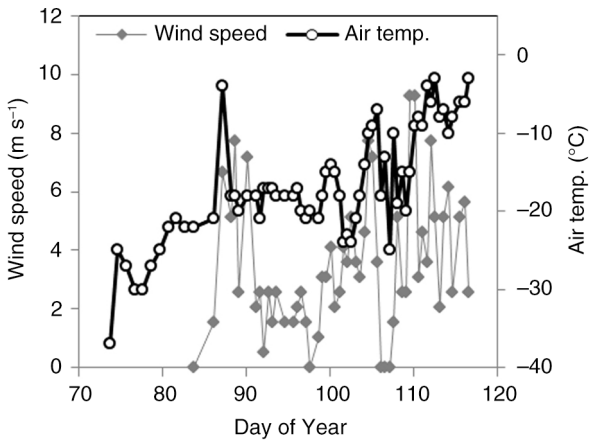

Fig. 2 Wind speed (m s^{-1}) and air temperature (°C) measured at the Catlin Ice Base (CIB) during March and April 2010.

local temperature minimum of −1.67°C at around 25 m. There was a second, warmer layer between 25 and 50 m with a maximum temperature of around −1.55°C. Below this layer, there was a strong thermocline from approximately 50 m to below 200 m. At the beginning of the period, there was a halocline from below 200 m to between 10 and 15 m. The salinity in this upper layer (1–10 m) increased during the 40-day period. The δO^{18} and salinity data indicated (as per, for example, Macdonald et al. 1995) that the fraction of meteoric water in the surface layer did not significantly change over the 40-day period ($R = 0.46$, $df = 9$, $p = 0.146$), whereas the decrease in the "ice-melt" fraction was significant ($R = 0.89$, $df = 9$, $p = 0.0002$), indicating that approximately 0.12 – 0.15 m of ice formed over the 40-day period, depending on the specific water mass end-members assumed.

The magnitude of the current velocity as measured with the ADCP showed a significant vertical shear in this area over the three-day deployment period (Fig. 4b, c) and that the strongest observed currents were in the layer between 15 and 30 m, corresponding to the minimum temperature layer observed in Fig. 3a. Additionally maximum speeds related to a southerly (south to south-west) flowing current, which was amplified during the tidal ebb (Fig. 4c). Depth and time-averaged (6–45 m and 15 min) currents indicate flow rates varying between 0.02 and 0.05 m s^{-1}. The observed currents were predominantly tidally generated, as can be seen in Fig. 4b, where these averaged current speeds are plotted with the local tidal elevation derived by the WebTide tidal projection model.

CIB chlorophyll

Surface seawater chlorophyll concentrations increased from an average 0.39 mg m^{-3} at the beginning of our study to 0.73 mg m^{-3} at the end ($R = 0.429$, $df = 42$, $p = 0.0036$; Fig. 5). This increase was most significant immediately below the ice ($R = 0.714$, $df = 10$, $p = 0.014$). Chlorophyll concentration did not show a significant correlation to nitrate + nitrite concentration ($R = 0.033$, $df = 42$, $p = 0.8308$), but there was a small, yet significant correlation with silicate ($R = 0.310$, $df = 42$, $p = 0.0402$) and with phosphate ($R = 0.336$, $df = 42$, $p = 0.0257$). Mean chlorophyll concentration in the upper 10-m water column also had a significant correlation with day length ($R = 0.609$, $df = 10$, $p = 0.0355$).

The chlorophyll concentration in the ice core melts was low in the top and middle sections (< 0.5 mg m^{-3}) but was significantly higher in the bottom section (Table 2). The below-ice seawater concentrations for the dates around those on which the ice cores were collected were also lower than those in the bottom core melts.

CIB inorganic nutrients

Nitrate + nitrite concentration was low (< 1.5 μM) in the upper 10 m, and there was no significant change in the concentrations through the field season. Nitrate increased with depth to about 12 μM at 100 m, while nitrite decreased (Fig. 5). Phosphate, ammonium and silicic acid all showed small, yet significant, decreases through the field season in the surface 10 m (phosphate: $R = 0.380$, $df = 42$, $p = 0.0105$; ammonium: $R = 0.411$, $df = 42$, $p = 0.0056$; silicate: $R = 0.299$, $df = 42$, $p = 0.0485$). Ammonium concentration was < 0.7 μM in the upper 10 m at the beginning of the sampling period but decreased to a minimum of 0.22 μM by 26 April. Phosphate concentration was ≤ 0.8 μM in the upper 10 m, increasing to just over 1 μM below 100 m, but decreased again at 200 m (Fig. 5). Silicate concentration was approximately 6 μM in the upper 10 m and increased to > 20 μM below 100 m (Fig. 5). None of the inorganic nutrients showed significantly different results when normalized to salinity ($S = 30.1$). The average difference between non-normalized and salinity-normalized nutrients was less than 0.15% of the original value (i.e., < 0.0015 μM difference between normalized nitrate + nitrite and non-normalized nitrate + nitrite).

The meltwater from the ice cores had lower concentrations of nitrite, silicate and phosphate than the seawater (Table 2). Nitrate concentration was higher than the seawater concentration at the surface of the ice, but nitrate and nitrite concentrations both decreased from top to bottom, while silicate and phosphate showed either no change or a small increase, respectively, through the ice core (Table 2).

Citation: *Polar Research* 2015, *34*, 24170, http://dx.doi.org/10.3402/polar.v34.24170

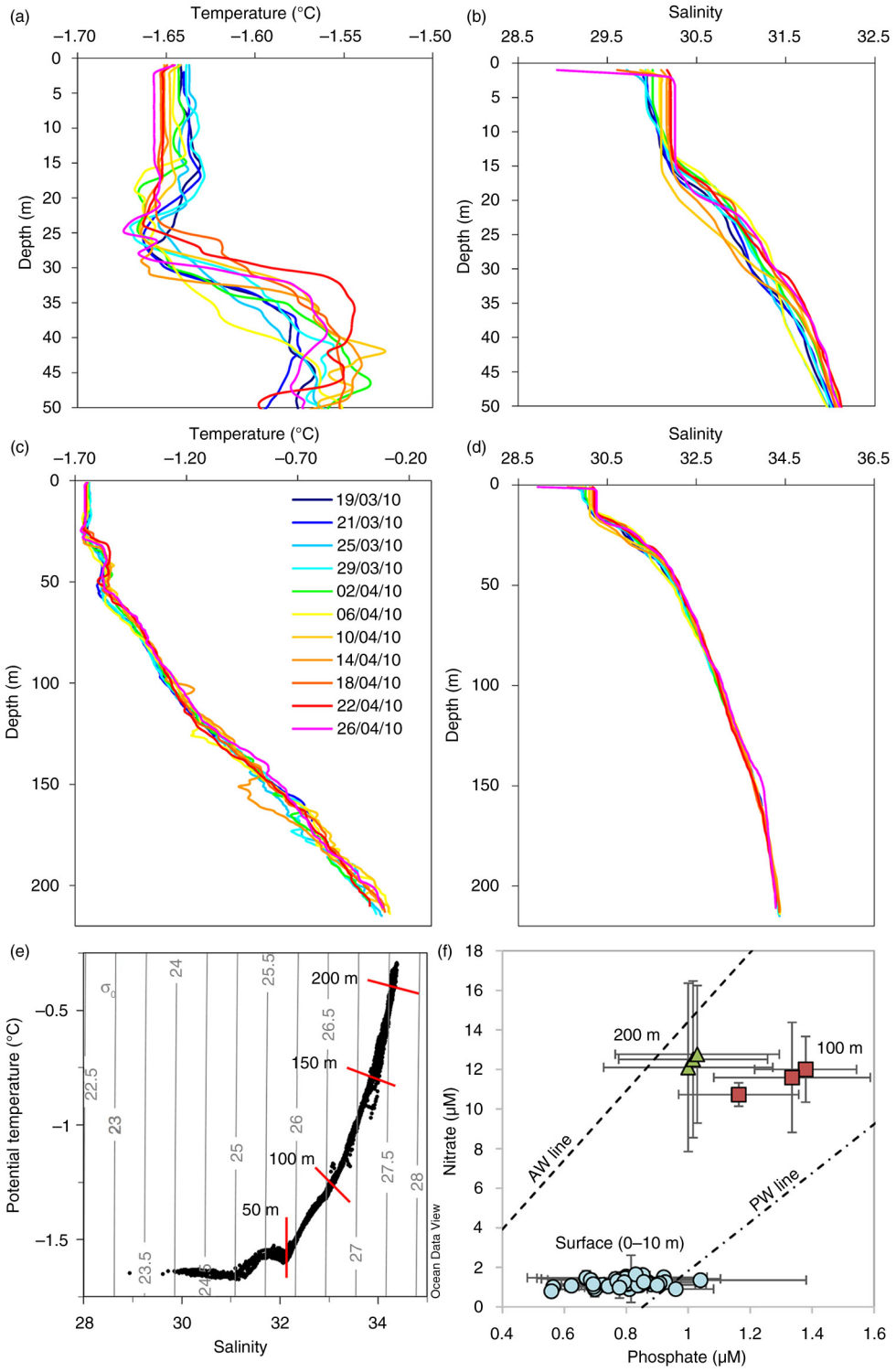

Fig. 3 Under the sea-ice water column profiles through the field campaign from 17 March to 26 April 2010 (different colours represent the different sample dates) for (a) 0 to 50 m temperature, (b) 0 to 50 m salinity, (c) 0 to 220 m temperature and (d) 0 to 220 m salinity. (e) Potential temperature versus salinity plots, overlaid with isopycnals, for all data from the full depth profiles, also highlighting every 50 m depth. (f) Nitrate versus phosphate concentrations (mean ± 1 SD) for each depth over the field campaign, also showing the PO_4 versus NO_3 regression lines expected for Atlantic Water (AW) and Pacific Water (PW; from Jones et al. 1998).

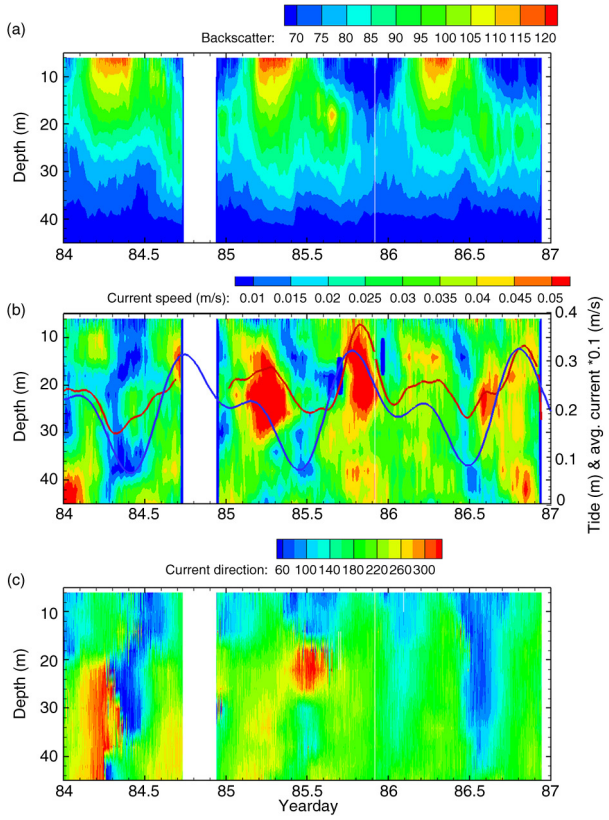

Fig. 4 (a) Uncalibrated acoustical backscatter intensity data from the 300-kHz acoustic doppler current profiler deployed for three days beneath the ice; (b) current speeds from the same instrument, showing significant variability and vertical shear, overlying lines indicate tidal elevation from the Webtide model (solid blue line) and current speeds averaged over the top 45 m and over 15 min (solid red line); and (c) current direction from the same instrument (degrees).

CIB inorganic carbon

Total alkalinity (A_T) was uniform through the upper 10 m, with little change through time. Total inorganic carbon (C_T) was also uniform throughout the upper 10 m but increased slightly through time ($<20\,\mu mol\,kg^{-1}$). This increase was not present when C_T was normalized to a constant salinity (nC_T, $S=30.1$). The calculated carbonate parameters within the seawater also did not vary through the top 10 m nor through time ($pH_T = 8.143 \pm 0.027$; $\Omega_{calcite} = 2.19 \pm 0.132$; $\Omega_{aragonite} = 1.36 \pm 0.082$). Both C_T and A_T increased with depth (Fig. 5; $C_T = 2188 \pm 4\,\mu mol\,kg^{-1}$ at 100 m and $2203 \pm 4\,\mu mol\,kg^{-1}$ at 200 m; $A_T = 2265 \pm 1\,\mu mol\,kg^{-1}$ at 100 m and $2298 \pm 3\,\mu mol\,kg^{-1}$ at 200 m). The pH and the $CaCO_3$ saturation states (aragonite and calcite) decreased with depth to 100 m but increased slightly again between 100 m and 200 m (Fig. 5). At the sampled depths, neither calcite nor aragonite became undersaturated, although $\Omega_{aragonite}$ approached 1 at 100 m.

The meltwater from the ice cores had much lower concentrations of C_T and A_T than the seawater (Table 2). When normalized to a constant salinity ($S=30.1$) to remove the effects of dilution, the meltwater had a lower concentration of nC_T than the surface seawater, particularly in the bottom and top ice sections. There was little difference in nA_T between the surface seawater and the bottom and mid-sections, although nA_T was reduced in the top section of the core.

The calculated seawater pCO_2 (pCO_{2SW}) again did not vary significantly within the upper 10 m or with time (mean $\pm$ SD $= 287 \pm 14\,\mu atm$). The surface water was significantly undersaturated with respect to atmospheric pCO_2 as measured by the ECS (pCO_{2atm}; $393 \pm 1\,\mu atm$), which was recorded only at the end of the sample period (25 to 29 April 2010, DoY 114 – 118; Fig. 5). Data from the atmospheric monitoring station at Alert on Ellesmere Island show that pCO_{2atm} at that site during the CIB field period ranged from 393.0 to 399.6 µatm (Dlugokencky et al. 2015), in good agreement with our limited data from the ECS.

The CO_2 ECS measured only small daily median fluxes ranging between -0.014 and $0.002\,\mu mol\,CO_2\,m^{-2}\,s^{-1}$, with an overall average of 0.027 ± 0.241 µmol (full measurement range of -1.00 to $1.32\,\mu mol$) $CO_2\,m^{-2}\,s^{-1}$ (where negative numbers indicate uptake of atmospheric CO_2 by the ice) from 25 to 28 April. The fluxes appeared to switch from a small release to a small uptake (Table 3) over those four days, but the fluxes were not statistically different from zero.

Spatial transect from 85°N to 90°N

Between 85 and 87°N, the polar surface water had salinities ranging from 29.3 to 30.4 (Fig. 6). A profile to approximately 65 m at the southernmost sampling location showed a halocline starting at 40 m (Fig. 6). Moving northwards into the Amundsen Basin, the salinity in the upper 30 m increased to over 31.5 (Fig. 6).

Chlorophyll concentration was $<0.2\,mg\,m^{-3}$ at all sites and decreased north of 86°N. The nutrient concentrations increased northwards, for example, nitrate increased from $<1\,\mu mol\,L^{-1}$ at 85°N to $>5\,\mu mol\,L^{-1}$at the North Pole (Fig. 7). Both C_T and A_T also generally increased towards the North Pole, from 1981 µmol kg^{-1} and 2082 µmol kg^{-1} at 85°N to 2118 µmol kg^{-1} and 2215 µmol kg^{-1} at the North Pole for $C_T$and A_T, respectively (Fig. 7). Normalized $C_T$and A_T ($S=30.1$) showed no change along the transect. C_T and A_T concentrations on the southern end of the CET transect, between 85 and 87°N (Fig. 7), were similar to those at the CIB off Ellef Ringnes Island (Fig. 5). Nitrate, silicate and phosphate concentrations at all CET sampling locations were

Citation: *Polar Research* 2015, *34*, 24170, http://dx.doi.org/10.3402/polar.v34.24170

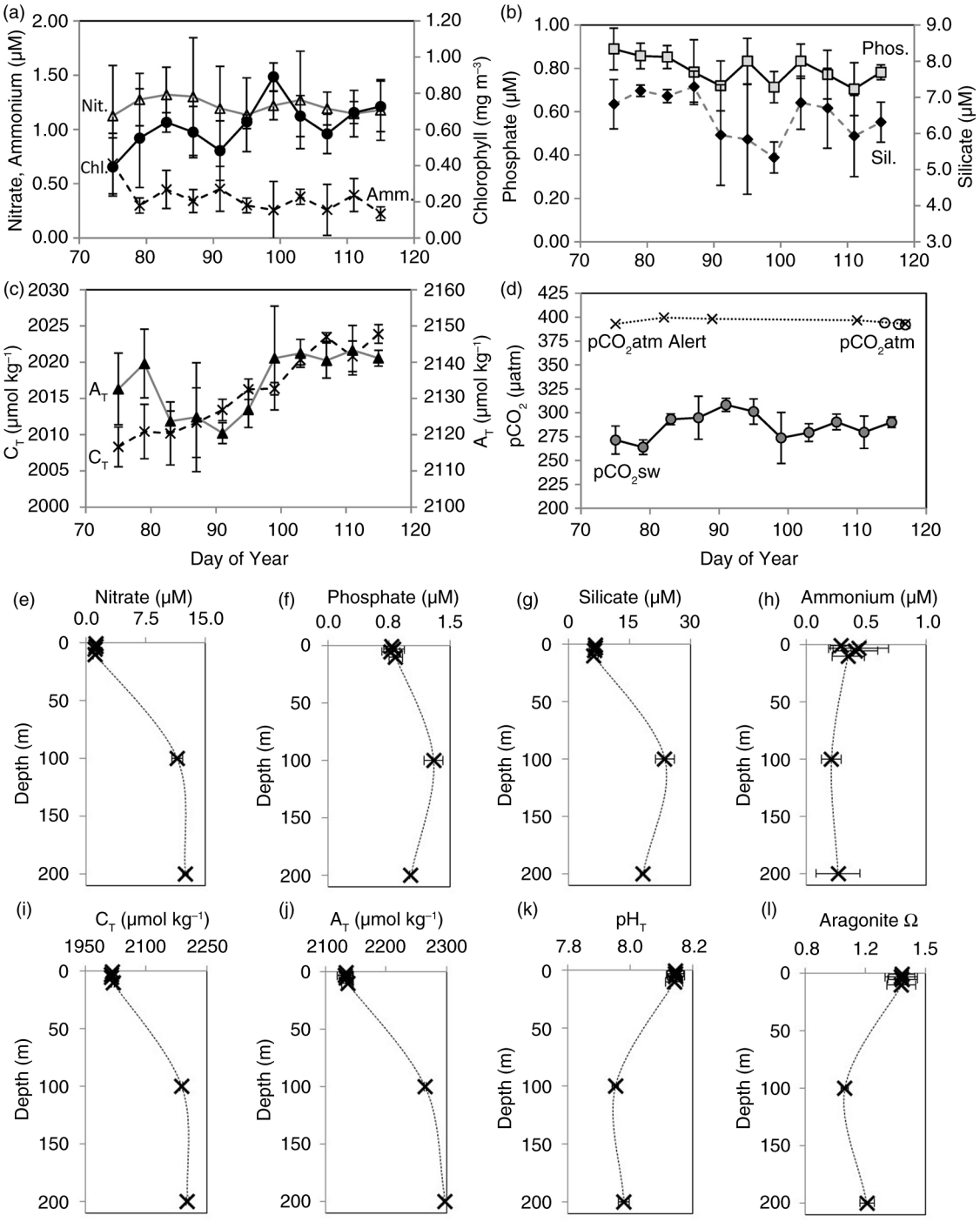

Fig. 5 (a–d) Average (mean) surface conditions (1 to 10 m of seawater) through the sampling period for (a) nitrate (µM), ammonium (µM) and chlorophyll (mg m^{-3}), (b) phosphate (µM) and silicate (µM), (c) total inorganic carbon (C_T, µmol kg^{-1}) and total alkalinity (A_T, µmol kg^{-1}) and (d) seawater pCO_2 (pCO_2sw), atmospheric pCO_2 (pCO_2atm) measured at the ice base by the eddy covariance system and pCO_2 from the Alert weather station (pCO_2atm Alert, [Dlugokencky et al. 2015]). (e–l) Average depth profiles for (e) nitrate, (f) phosphate, (g) silicate, (h) ammonium, (i) total inorganic carbon concentration (C_T), (j) total alkalinity (A_T), (k) pH_T and (l) aragonite saturation state (aragonite Ω). The error bars represent ±1 standard deviation.

similar to the measurements taken at the CIB, except for the northernmost sites, where the concentrations increased significantly.

Across the CET under-ice pCO_{2sw} was consistently lower than the pCO_{2atm}, with a general decrease away from the Canadian coast, until reaching 88°39 N when the pCO_{2sw}

Table 2 Biogeochemical measurements averaged across all ice cores for each section (top, middle and bottom). Values are mean ± standard deviation.

	Top section	Middle section	Bottom section
Sal.	8.8 ± 1.1	5.68 ± 0.7	5.19 ± 0.8
Nitrite (μM)	0.06 ± 0.01	0.05 ± 0.02	0.03 ± 0.01
Nitrate (μM)	1.15 ± 0.34	0.40 ± 0.15	0.32 ± 0.14
Phosphate (μM)	0.11 ± 0.03	0.11 ± 0.04	0.19 ± 0.13
Silicate (μM)	1.35 ± 0.20	1.05 ± 0.35	1.26 ± 0.21
Ammonium (μM)	0.61 ± 0.08	0.56 ± 0.16	0.52 ± 0.32
Chl (mg m^{-3})	0.21 ± 0.13	0.32 ± 0.28	2.21 ± 0.911
A_T (μmol kg^{-1})	569 ± 62	402.3 ± 54.75	369.3 ± 56.29
C_T (μmol kg^{-1})	508 ± 40	374.7 ± 44.05	325.2 ± 51.05

increased again (pCO_{2sw} ranged from 241.5 μatm to 368.1 μatm). Surface water (1–10 m) pH_T ranged between 8.05 and 8.15 across the transect, following a reverse pattern to pCO_2, as expected. Neither aragonite nor calcite was undersaturated in the surface water under the ice, although the aragonite saturation state was <1.3 near the coast but increased towards the North Pole.

Discussion

We found that the biogeochemical conditions in the water column under the sea ice during late winter in the outer regions of the Canadian Arctic Archipelago were more similar to surface conditions of the offshore Arctic Ocean than what has been observed in the past in the centre of the archipelago (e.g., Mundy et al. 2014). Specifically, the conditions at our ice base off Ellef Ringnes Island were similar to the low-nutrient waters of the multi-year ice-covered Canada Basin (Else et al. 2013). There was relatively little change in the water column conditions under the ice over the sampling period, with a strong halocline starting at about 15 m, again similar to the shallow winter mixed layer depths found in the Canada Basin (Toole et al. 2010). The temperature and salinity data, together with the nutrient data, showed that the water in the surface down to 100 m is representative of Pacific water, transitioning towards Atlantic water near 200 m (Fig. 3f), as would be expected from previous work (Jones et al. 1998). The dominant current flow was in a southerly direction, and the anticyclonic circulation pattern that is prevalent in the central Arctic at this time of year tends to transport water along the shelf from regions dominated by multi-year ice (Proshutinsky & Johnson 2001). In line with previous observations, the surface mixed layer depth at the CIB appears to vary little, on account of dampened mixing regimes and horizontal advection processes (Prinsenberg & Ingram 1991; Carmack & Wassmann 2006; Toole et al. 2010).

During the study period, sea ice was still forming, which increased salinity in the surface waters. Despite this salinity increase, the mixed layer depth remained relatively shallow, ranging from 10 to 18 m, and this inhibited deepening appeared to prevent significant replenishment of nutrients and carbon into the near-surface waters. Indeed, we found considerably low nutrient concentrations, as well as low C_T and A_T resulting in low seawater pCO_2 conditions, in the surface mixed layer throughout the study period. Furthermore, although there was a significant detectable increase in chlorophyll in the surface waters, which correlated with an increase in day length, we caution that there was no corresponding removal of nitrate + nitrite or carbon (even when normalized to salinity) and that the increase is relatively small compared to other observed ice algae and under-ice blooms (e.g., chlorophyll >10 mg m^{-2}; Mundy et al. 2014). The under-ice conditions we observed therefore suggest that there may not be sufficient nutrient levels in the northern reaches of the archipelago to instigate or sustain a large bloom as the light continues to increase.

The Canadian High Arctic shelf region

The nutrient concentrations observed in this study are generally smaller than those observed previously in winter Arctic surface waters, for example: average NO_3 at the CIB = 1.5 μmol L^{-1}; station T3, Canada Basin: NO_3 = 5.6 μmol L^{-1} (Kinney et al. 1970); station CESAR, central Arctic (Alpha Ridge): NO_3 = 4.8 μmol L^{-1} (Jones & Anderson 1986); Resolute: NO_3 = 6.5–10.0 μmol L^{-1} (Cota et al. 1987); Barrow, Alaska: NO_3 = 6.5–7.3 μmol L^{-1} (Lee et al. 2008); Franklin Bay: NO_3 = 2.0–6.0 μmol L^{-1} (Tremblay et al. 2008). If biological consumption was the only process influencing removal of nitrate, a reduction in nitrate from "normal" wintertime conditions of

Table 3 Data from CO_2 eddy covariance system. Median values ± standard error. Positive values for fluxes of sensible heat/CO_2 indicate transport of heat/CO_2 away from surface into the atmosphere

Date	Air temp. (°C)	V.P.[a] (kPa)	W.S.[b] ($m.s^{-1}$)	CO_2 [c] (ppm)	S.H.F.[d] ($W.m^{-2}$)	CO_2 flux ($\mu mol.m^{-2}.s^{-1}$)
25/04/10	−11.6 ± 0.16	1.09 ± 0.011	5.80 ± 0.08	394.0 ± 0.27	−16.4 ± 1.47	0.0021 ± 0.0467
27/04/10	−8.3 ± 0.17	1.28 ± 0.010	3.88 ± 0.16	392.5 ± 0.21	0.7 ± 0.64	0.0006 ± 0.0307
28/04/10	−16.2 ± 0.33	1.03 ± 0.011	4.36 ± 0.22	392.2 ± 0.21	1.1 ± 0.77	−0.0144 ± 0.0198

[a]Vapour pressure. [b]Wind speed. [c]Atmospheric CO_2 concentration. [d]Sensible heat flux.

Citation: *Polar Research* 2015, *34*, 24170, http://dx.doi.org/10.3402/polar.v34.24170

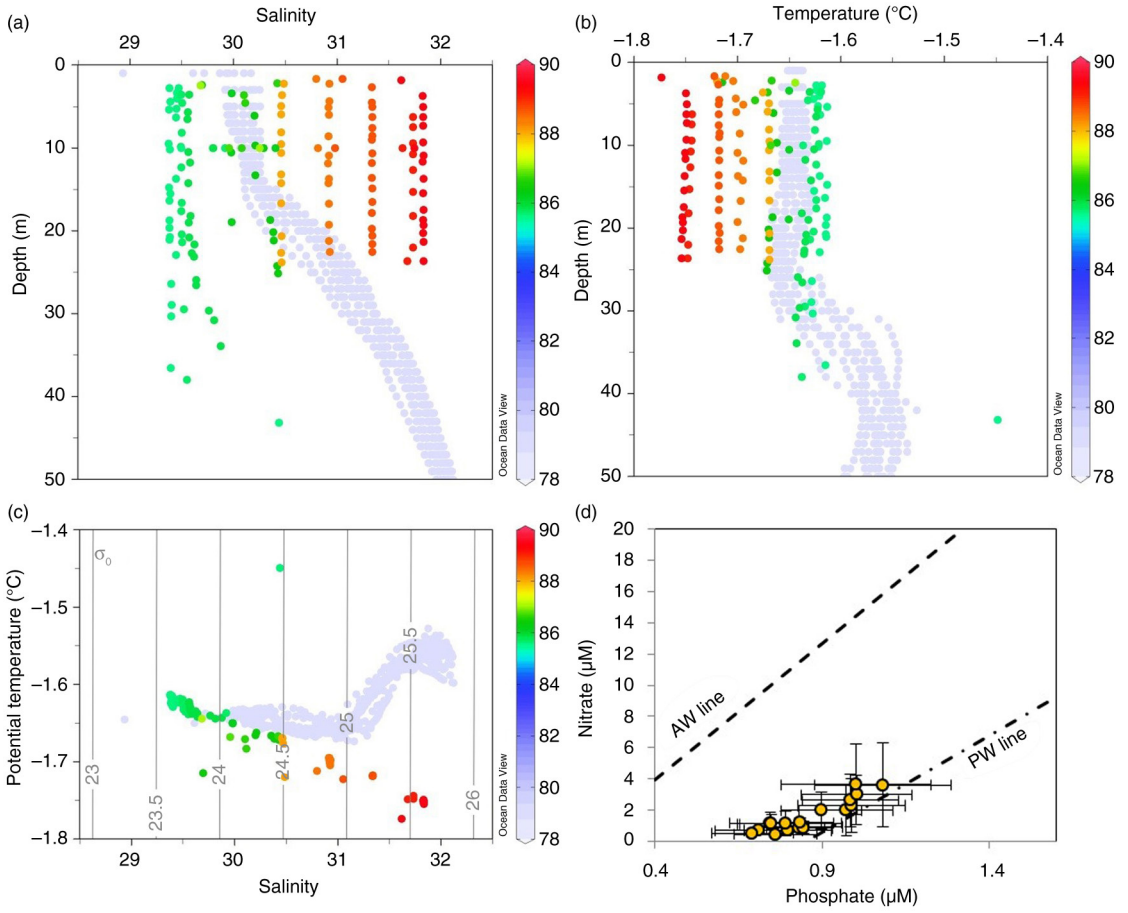

Fig. 6 Water column profiles at each latitude (shown as different colours) from the Catlin Explorer Transect for (a) salinity and (b) temperature; (c) potential temperature vs salinity plot for the upper 50 m, overlaid with isopycnals. Each figure also shows the upper 50 m Catlin Ice Base data as a comparison (light blue, 78°N). (d) Nitrate versus phosphate concentrations (mean ± 1 SD) for surface (0 – 10 m) over the transect, also showing the PO_4 vs NO_3 regression lines expected for Atlantic Water (AW) and Pacific Water (PW; from Jones et al. 1998).

5–10 μmol L^{-1} to the observed concentration of 1.27 μmol L^{-1} would require a chlorophyll bloom of >3.73 mg m^{-3} to have occurred prior to 17 March, which seems extremely unlikely because of low light levels and short day lengths. The relatively low nutrient concentrations in the surface waters at the beginning of our study therefore suggest that replenishment of surface nutrients by mixing (winter internal mixing or horizontal advection [e.g., Carmack & Wassmann 2006]) had not occurred to a significant extent in this area. Furthermore, there was no significant difference between the nutrient data and salinity-normalized nutrient data, suggesting that brine rejection and ice formation-related mixing events (Prinsenberg & Ingram 1991; Toole et al. 2010) also had not contributed significant amounts of nutrients to the surface layer during this period. Furthermore, the low NO_3^-:P ratios in the surface water (NO_3^-:$P<2$) suggests a decoupling in the renewal processes of these different nutrients over winter, similar to what was found by Tremblay et al. (2008) at another entrance to the Canadian Arctic Archipelago, in the south-eastern Beaufort Sea. The high Si:NO_3^- ratio in the surface waters (Si:NO_3^- >7), again a signature of a nutrient-depleted system, also supports the hypothesis that this system, surrounded by multi-year ice, has reduced wintertime nutrient replenishment.

Despite the low nutrient concentrations, we did detect a small increase in chlorophyll: the integrated surface water (1–10 m) chlorophyll increased from 1.19 mg m^{-2} to 2.94 mg m^{-2} during the 40-day period, resulting in a chlorophyll-calculated growth rate of 0.044 day^{-1}. Gilstad & Sakshaug (1990) assessed phytoplankton growth rates under a range of day lengths and light conditions and showed that with just four hours of daylight, the average diatom growth rate (of 10 diatoms sp.) was 0.05 day^{-1}. However, we note that diatoms are

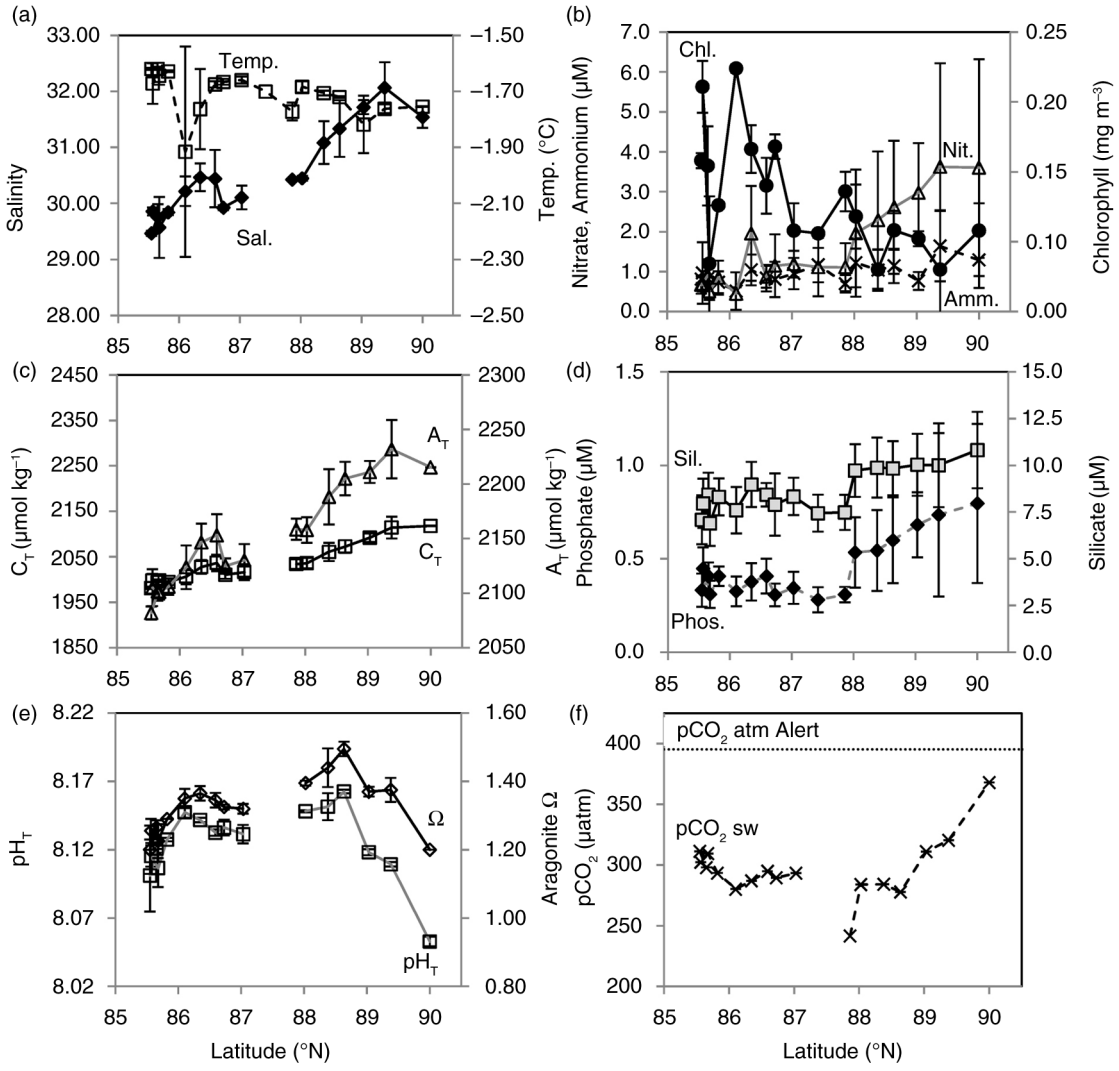

Fig. 7 Average (mean ± 1 SD) surface (0 to 10 m) seawater conditions under the sea ice along the Catlin Explorer Transect from 85°N to the North Pole for (a) salinity and temperature (°C); (b) chlorophyll (mg m^{-3}), ammonium (µM) and nitrate (µM); (c) total inorganic carbon (C_T, µmol kg^{-1}) and total alkalinity (A_T, µmol kg^{-1}); (d) phosphate and silicate (µM); (e) pH (total scale) and aragonite saturation state (aragonite Ω) and (f) pCO_2 of seawater, also showing the average atmospheric pCO_2 measured at Alert Station over the duration of the transect (pCO_2atm Alert [Dlugokencky et al. 2015]).

unlikely to be the dominant phytoplankton group under the ice at this time of year, with picoplankton flagellates more likely the key component of the community instead (Lovejoy et al. 2007). Eilertsen et al. (1989) suggested that primary production can occur at relatively low light levels in the Arctic Ocean, and our observations support this. Similarly, small increases in chlorophyll have been observed around the Arctic at the same time of year (Cota et al. 1987; Lovejoy et al. 2007), predominantly as a result of the over-winter persistence and subsequent growth of picoplankton (Lovejoy et al. 2007).

The observed increase in chlorophyll under the ice would have a nutrient demand of approximately 0.045 mmol m^{-2} day^{-1}, or >1.75 mmol m^{-2} over the 40-day period (assuming roughly 1 mmol m^{-3} nitrate is required for 1 mg Chl m^{-3} [M. Gosselin, pers. comm.]). As nitrate + nitrite (even when normalized to salinity) did not show a significant decrease nor a significant relationship with chlorophyll, the observed changes in nitrate + nitrite concentration cannot explain the changes in chlorophyll. This small nutrient demand (1.75 mmol m^{-2} or 0.2 umol L^{-1} N addition) is well within the observed variability of daily measured nitrate + nitrite and therefore simply may not be detectable here. Ammonium concentration did show a slight decrease in concentration through the study period, as well as a significant negative

Citation: *Polar Research* 2015, *34*, 24170, http://dx.doi.org/10.3402/polar.v34.24170

correlation with chlorophyll; however, there may be problems with measuring ammonium from stored samples, so cautious interpretation of these results are required. That said, it seems plausible that ammonium, through nutrient recycling, could be a dominant nitrogen source in this area; further work is required to confirm this.

Alternatively, Cota et al. (1987) estimated nutrient fluxes ranging from 0.5 to 3 mmol m^{-2} day^{-1} (distributed through the 10-m surface water column) resulting from tidal mixing from below the pycnocline. Their tidal mixing model may be reasonable for the CIB in view of the clear tidal influence on water motions at our study site (Fig. 4). Cota et al. (1987) measured larger tidal flows in April through June in the central archipelago, than we did at our study site, which was likely influenced by the winter ice dampening effect (Prinsenberg & Ingram 1991). Based on the vertical profile of nitrate (concentration in surface 10 m and below the pycnocline at 100 m) and tidal data from the tidal station at Isachsen (Ellef Ringnes Island, Nunavut/Northwest Territory 103°32.00′W, 78° 47.00′N), we estimate that vertical mixing of nitrate into the surface waters would be on the order of 0.042 mmol m^{-2} day^{-1}. Therefore, tidally driven nitrate fluxes could have provided a proportion of the nutrient demand, together with regenerated nutrients.

However, our findings temper the idea that large under-ice phytoplankton blooms are a widespread, yet under-documented, phenomenon in polar regions (Mundy et al. 2009) because a larger bloom could not be sustained with these low-nutrient conditions. Although both Arrigo et al. (2012) and Mundy et al. (2014) have found substantial under-ice phytoplankton blooms in the Arctic Ocean (phytoplankton biomass >1000 mg C m^{-3} in shallow shelf in the Chukchi Sea and 508 mg Chl m^{-2} in the inner Canadian Arctic Archipelago, respectively), their observations were later in the season (May–July) and in areas with higher initial nutrient concentrations than those found in our study area.

Measured C_T and A_T were low at the surface (1–10 m) compared to other oceanic regions (Fig. 5), although they were within ranges of other summertime data from the Canadian Arctic Archipelago (e.g., Miller et al. 2002; Chierici & Fransson 2009; Azetsu-Scott et al. 2010). The few late-winter inorganic carbon data that are available show pre-bloom, under-ice C_T and A_T concentrations to be higher than the values observed here. On average across the surface 10 m at the CIB, we found $C_T = 2015$ μmol kg^{-1} and $A_T = 2134$ μmol kg^{-1}, while others have found values of 2150–2180 μmol kg^{-1} for C_T and 2250–2260 μmol kg^{-1} for A_T in the south-eastern Beaufort Sea in March and April (Rysgaard et al. 2007; Miller et al. 2011). The CIB values presented here are consistently lower than other high-latitude wintertime values even after taking into account differences in salinity (i.e., by normalizing to the same salinity). Wintertime concentrations are generally expected to increase in surface waters under sea ice, as a result of rejection of carbon with brine extrusion during sea-ice formation (Miller et al. 2011). Some increase in C_T was evident at the CIB with the increase in salinity, but increases due to organic matter remineralization were not apparent (Junge et al. 2004). There is no correlation between normalized C_T and chlorophyll, which suggests that photosynthesis did not significantly contribute to CO_2 consumption in our study area or at least has consumed CO_2 in balance with the addition of CO_2 from respiration.

The C_T and A_T concentrations of the meltwater from the ice cores were similar to measurements from ice cores of melted first-year sea ice in Franklin Bay, Canada; Young Sound, Greenland; and the Canadian Basin (Anderson & Jones 1985; Rysgaard et al. 2007; Miller et al. 2011) suggesting similar carbon cycling processes occur in the sea ice as at least across the western Arctic. The values of nC_T were significantly lower at the top of the ice, which may indicate CO_2 loss from the ice to the atmosphere at some time since the ice first began to form.

Not surprisingly, in view of the extremely low temperatures (and presumably, associated low brine volumes within the sea ice), the CO_2 flux observed here (-0.0014 to 0.0021 μmol m^{-2} s^{-1} = -0.12 to 0.18 mmol m^{-2} day^{-1}) was much smaller than CO_2 fluxes measured by ECS in other sea-ice-covered areas, which range from -212 to $+86$ mmol m^{-2} day^{-1} (Semiletov et al. 2004; Zemmelink et al. 2006; Miller et al. 2011; Papakyriakou & Miller 2011), although high levels of variability have been found on hourly and daily timescales (Miller et al. 2011; Papakyriakou & Miller 2011). The CO_2 fluxes measured over ice-covered areas appeared to be about an order of magnitude smaller than fluxes observed over open leads and polynyas during ice formation (-431 to $+250$ mmol m^{-2} day^{-1} [Else et al. 2011]), where the fluxes were predominantly directed towards the water. Therefore, because of the relatively low pCO_2 under the ice in our study—lower than other recorded winter and early spring values (Miller et al. 2011; Papakyriakou & Miller 2011)—we could expect a rapid CO_2 uptake from the atmosphere into the ocean, if the shear zone between drifting ice and the stationary, land-fast ice developed into flaw leads and polynyas, a phenomenon typical of this area of the Arctic (Carmack & Wassmann 2006).

A pH_T, calcite and aragonite saturation state minimum occurred in this data set at around 100 m. This mid-water column minimum in pH_T and saturation state has also been observed in the Arctic Ocean on a number of

previous occasions and was thought to exist because of remineralization of organic matter either directly in the subsurface layer or through vertical transport (seasonal upwelling events) of carbon (Bates et al. 2009; Shadwick et al. 2011; Lansard et al. 2012; Mathis et al. 2012). Although the observations by Bates et al. (2009) and Mathis et al. (2012) were only made in the spring or summer periods and were thought to be a seasonally induced phenomenon (Bates et al. 2009). Shadwick et al. (2011) and Lansard et al. (2012) confirmed that the phenomenon persists throughout the winter, which is consistent with the results from this study.

The central Arctic Ocean

With the CIB located on the continental shelf (Fig. 1a), the biogeochemical dynamics could be influenced by land- and/or sediment-associated processes, as well as shallow mixing dynamics (Prinsenberg & Ingram 1991) and may not be representative of conditions offshore, in the central basin of the Arctic Ocean. Therefore, the Catlin Arctic Survey also collected samples along a transect—the CET—from above the north coast of Ellesmere Island towards the North Pole (Fig. 1b). The CET crossed the Makarov Basin (water depth >1000 m), over the Lomonosov Ridge and into the Amundsen Basin (water depth >4000 m), thus crossing Pacific-influenced water masses, similar to those expected to enter the Canadian Arctic Archipelago near the CIB (Jones et al. 1998) and exemplified by the surface nutrient data from the CET closely following the phosphate–nitrate relationship described by Jones et al. (1998), as illustrated in Fig. 6d.

Nitrate, phosphate, silicate and C_T concentrations measured on the CET (Fig. 7) were all lower than those observed during April and May at the CESAR ice camp (established in March 1983 at 85.75°N, 111.0°E) in the surface waters under the sea ice (Jones & Anderson 1986), although north of 88°N, the concentrations we measured approached those observed during the early spring at CESAR and also those at the LOREX ice camp (April and May 1979 from 88.67°N, 139.83°W to 89.15°N, 97.12°W [Moore et al. 1983]). The observations most similar to the CIB data were found at the southern end of the CET, between 85 and 87°N. The increase in concentrations at the higher latitudes (>88°N) corresponds to samples that were taken over the Lomonosov Ridge and into the much deeper, more Atlantic-influenced Amundsen Basin, characterized by more saline surface waters. In this region, stronger mixing processes may be prevalent, which would contrast with the dynamics closer to the Canadian shelf, where mixing processes did not appear sufficient to entrain new nutrients into the surface water.

This transect data set is complicated by spatial and temporal covariation, as is the case for many shipboard studies. Although day length increased rapidly over the first few weeks of the expedition, there were also variations in sea-ice thickness and snow cover between sampling locations (Table 4). Water column chlorophyll concentration was negatively correlated with snow thickness, although not significantly ($df = 17$, $R = 0.3961$, $p = 0.0932$), but was significantly negatively correlated with ice thickness ($df = 17$, $R = 0.4712$, $p = 0.0417$).

The $CaCO_3$ saturation states (calcite and aragonite) in the surface waters across the whole transect were, in general, lower than previously observed spring and summer surface water conditions for other areas of the Arctic Ocean (e.g., Bates et al. 2009). Although different drivers are likely to contribute to these low wintertime pH_T and saturation state conditions than drivers in more southerly locations, these data confirm the hypothesis that winter pH_T and saturation states in surface waters will be lower than those during the productive summer and spring seasons (Findlay et al. 2008; Bates et al. 2009; Olafsson et al. 2009). The CET data set provides spatial evidence that moving offshore towards the central Arctic, late winter aragonite saturation states in the surface layers are <1.5 and beyond 88.5°N actually decrease in the surface 10 m to ca. 1.2; pH_T also decreases from approximately 8.15 between 86 and 88.5°N to 8.05 at the North Pole. Together with profile data from the CIB, the CET

Table 4 Catlin Explorer Transect sample information: date, location (latitude and longitude), snow thickness and ice thickness.

Station	Date	Latitude	Longitude	Snow (cm)	Ice thickness (cm)
1	14/03/10	85°32′54″N	77°44′17″W	19.8	221.0
2	18/03/10	85°38′46″N	77°55′19″W	9.4	259.0
3	21/03/10	85°34′52″N	78°21′14″W	8.2	156.0
4	24/03/10	86°35′77″N	85°00′48″W	2.7	233.0
5	27/03/10	85°49′17″N	79°08′20″W	12.5	300.0
6	30/03/10	86°06′11″N	82°27′01″W	9.0	125.0
7	04/04/10	86°20′47″N	83°42′47″W	14.0	220.5
8	07/04/10	86°35′27″N	85°16′32″W	14.3	272.3
9	10/04/10	86°43′37″N	85°09′29″W	16.3	229.3
10	13/04/10	87°02′07″N	79°34′38″W	56.0	315.7
11	16/04/10	87°25′12″N	71°51′46″W	16.0	373.5
12	20/04/10	87°40′59″N	74°15′15″W	16.0	194.0
13	25/04/10	89°01′36″N	63°14′11″W	24.4	212.4
14	28/04/10	88°22′41″N	59°37′21″W	21.0	198.0
15	01/05/10	88°38′10″N	62°19′33″W	24.7	193.3
16	04/05/10	89°01′52″N	68°10′58″W	29.0	275.7
17	07/05/10	89°22′39″N	72°48′42″W	23.7	225.3
18	12/05/10	90°N		24.0	214.0

Citation: *Polar Research* 2015, *34*, 24170, http://dx.doi.org/10.3402/polar.v34.24170

data suggest that the relatively shallow (around 100 m) subsurface layers are likely already reaching undersaturation with respect to aragonite. Any upwelling events or internal mixing that drives this water onto the slopes and shelves (Williams et al. 2006; Mathis et al. 2007) would mean benthic communities there could already be exposed to year-round corrosive conditions.

Conclusions

The outer shelf and slope region north of the Canadian Archipelago is dominated by a mix of land-fast ice and pack ice, first- and multi-year ice, with polynyas, flaw leads and open ice areas occurring, which create new (first-year) ice. In these regions of sluggish circulation (low wind-driven mixing, dampened tidal dynamics and increased horizontal advection), the changes in salinity, driven by sea-ice formation, appears to be the main forces contributing to the surface water carbon, but not nutrient, dynamics under the sea ice prior to the onset of the spring–summer biologically productive period. The wintertime surface mixed layer was characterized by low C_T and A_T concentrations, resulting in waters undersaturated with respect to pCO_2 (285 µatm) with a surface water pH_T of 8.14 and aragonite $\Omega = 1.36$. pCO_2 increased with depth to a maximum of 476 µatm at 100 m, resulting in a pH of 7.95, and an aragonite $\Omega = 1.03$. Low NO_3^-:PO_4 but high Si:NO_3^- in the surface waters indicated that the CIB was nutrient-depleted and consequently even as light increases in spring, primary production could remain nutrient-limited in this region.

Acknowledgements

The Catlin Arctic Survey was funded by Catlin Ltd. and coordinated by Geo Mission Ltd. HSF was supported by the Plymouth Marine Laboratory Lord Kingsland Fellowship and received the Ralph Brown Expedition Grant from the Royal Geographical Society (with IBG) and a Royal Society Travel Grant. CL was supported by a Natural Environment Research Council (NERC) Fellowship (NE/G014728/1). LAE was supported by the NERC's National Centre for Earth Observation and received fieldwork funds from the World Wide Fund for Nature. LAM, GC and SV were supported by the Department of Fisheries and Oceans, Canada. The authors are extremely grateful to the Ice Base staff and Geo Missions support staff, especially A. Daniels, C. Paton and M. Hartley. We also express our thanks to E.M.S. Woodward at the Plymouth Marine Laboratory for nutrient analytical assistance, C. Michel from the Department of Fisheries and Ocean, Canada (Discovery Grant, Natural Sciences and Engineering Research Council of Canada) for lending us their ice corer and for advice on the data, M. Davelaar and K. Johnson at the Institute of Ocean Sciences for logistical and analytical assistance, M. Gosselin for advice on the chlorophyll and phytoplankton dynamics and B. Else and anonymous reviewers for their constructive advice. The data from this study are available from the British Oceanographic Data Centre, NERC (www.bodc.ac.uk/data/published_data_library/catalogue/10.5285/03167d6f-a9cc-2e1a-e053-6c86abc0753b/).

References

Anderson L.G. & Jones E.P. 1985. Measurements of total alkalinity, calcium, and sulphate in natural sea ice. *Journal of Geophysical Research—Oceans 90*, 9194–9198.

Arrigo K.R., Perovich D.K., Pickart R.S., Borwn Z.W., van Dijken G.L., Lowry K.E., Mills M.M., Palmer M.A., Balch W.M., Bahr F., Bates N.R., Benitez-Nelson C., Bowler B., Brownlee E., Ehn J.K., Frey K.E., Garley R., Laney S.R., Lubelczyk L., Mathis J., Matsuoka A., Micthell B.G., Moore G.W.K., Ortega-Retuerta E., Pal S., Polashenski C.M., Reynolds R.A., Schieber B., Sosik H.M., Stephens M. & Swift J.H. 2012. Massive phytoplankton blooms under Arctic sea ice. *Science 336*, 1408.

Aubinet M., Grelle A., Ibrom A., Rannik Ü., Moncrieff J., Foken T., Kowalski A.S., Martin P.H., Berbigier P., Bernhofer C., Clement R., Elbers J., Granier A., Grunwald T., Morgenstern K., Pilegaard K., Rebmann C, Snijders W., Valentini R. & Vesala T. 2000. Estimates of the annual net carbon and water exchange of forests: the EUROFLUX methodology. *Advances in Ecology Research 30*, 113–175.

Azetsu-Scott K., Clarke A., Falkner K., Hamilton J., Jones E.P., Lee C., Petrie B., Prinsenberg S., Starr M. & Yeats P. 2010. Calcium carbonate saturation states in the waters of the Canadian Arctic Archipelago and the Labrador Sea. *Journal of Geophysical Research—Oceans 115*, C11021, doi: http://dx.doi.org/10.1029/2009JC005917

Bates N.R. & Mathis J.T. 2009. The Arctic Ocean marine carbon cycle: evaluation of air–sea CO_2 exchanges, ocean acidification impacts and potential feedbacks. *Biogeosciences 6*, 2433–2459.

Bates N.R., Mathis J.T. & Cooper L.W. 2009. Ocean acidification and biologically induced seasonality of the carbonate mineral saturation states in the western Arctic Ocean. *Journal of Geophysical Research—Oceans 114*, C11007, doi: http://dx.doi.org/10.1029/2008JC004862

Brewer P.G. & Riley J.P. 1965. The automatic determination of nitrate in sea water. *Deep-Sea Research 12*, 765–772.

Brown K.A, Miller L.A., Mundy C.J., Papakyriakou T., Francois R., Gosselin M., Carnat G., Swystun K. & Tortell P.D. 2015. Inorganic carbon system dynamics in landfast Arctic sea ice during the early-melt period: spring sea ice inorganic carbon system. *Journal of Geophysical Research—Oceans 120*, 3542–3566.

Carmack E. & Wassmann P. 2006. Food webs and physical–biological coupling on pan-Arctic shelves: unifying concepts and comprehensive perspectives. *Progress in Oceanography 71*, 446–477.

Chierici M. & Fransson A. 2009. Calcium carbonate saturation in the surface water of the Arctic Ocean: undersaturation in freshwater influenced shelves. *Biogeosciences 6*, 2421–2432.

Comiso J.C. 2003. Large-scale characteristics and variability of the global sea ice cover. In D.N. Thomas & G.S. Dieckmann (eds.): *Sea ice: an introduction to its physics, biology, chemistry, and geology*. Pp. 112–142. Oxford: Blackwell Science.

Cota G.F., Prinsenberg S.J., Bennett E.B., Loder J.W., Lewis M.R., Anning J.L., Watson N.H.F. & Harris L.R. 1987. Nutrient fluxes during extended blooms of Arctic ice algae. *Journal of Geophysical Research—Oceans 92*, 1951–1962.

Dickson A.G. 1990. Standard potential of the reaction: $AgCl_{(s)} + 1/2H_{2(g)} = Ag_{(s)} + HCl_{(aq)}$, and the standard acidity constant of the ion HSO_4^- in synthetic sea water from 273.15 to 318.15 K. *Journal of Chemical Thermodynamics 22*, 113–127.

Dickson A.G. & Millero F.J. 1987. A comparison of the equilibrium constants for the dissociation of carbonic acid in seawater media. *Deep-Sea Research 34*, 1733–1743.

Dickson A.G., Sabine C.L. & Christian J.R. (eds.) 2007. *Guide to best practices for ocean CO_2 measurements. PICES Special Publication 3*. Oak Ridge, TN: Carbon Dioxide Information Analysis Center, Oak Ridge National Laboratory, US Department of Energy.

Dlugokencky E.J., Lang P.M., Masarie K.A., Crotwell A.M. & Crotwell M.J. 2015. Atmospheric carbon dioxide dry air mole fractions from the NOAA ESRL Carbon Cycle Cooperative Global Air Sampling Network, 1968–2014. Version 2015-08-03. Boulder, CO: Earth System Research Laboratory, National Oceanic and Atmospheric Administration. Accessed on the internet at ftp://aftp.cmdl.noaa.gov/data/trace_gases/co2/flask/surface/ [Copyeditor: this does not require an internet access date]

Eilertsen H.C., Taasen J.P. & Weslawski J.M. 1989. Phytoplankton studies in the fjords of west Spitzbergen: physical environment and production in spring and summer. *Journal of Plankton Research 11*, 1245–1260.

Else B.G.T., Galley R.J., Lansard B., Barber D.G., Brown K., Miller L.A., Mucci A., Papakyriakou T.N., Tremblay J.-E. & Rysgaard S. 2013. Further observations of a decreasing atmospheric CO_2 uptake capacity in the Canada Basin (Arctic Ocean) due to sea ice loss. *Geophysical Research Letters 40*, 1132–1137.

Else B.G.T., Papakyriakou T.N., Galley R.J., Drennan W.M., Miller L.A. & Thomas H. 2011. Wintertime CO_2 fluxes in an Arctic polynya using eddy covariance: evidence for enhanced air–sea gas transfer during ice formation. *Journal of Geophysical Research—Oceans 116*, C00G03, doi: http://dx.doi.org/10.1029/2010JC006760

Findlay H.S., Tyrrell T., Bellerby R.G.J., Merico A. & Skjelvan I. 2008. Carbon and nutrient mixed layer dynamics in the Norwegian Sea. *Biogeosciences 5*, 1395–1410.

Flato G.M. & Brown R.D. 1996. Variability and climate sensitivity of landfast Arctic sea ice. *Journal of Geophysical Research—Oceans 101*, 25767–25777.

Gilstad M. & Sakshaug E. 1990. Growth rates of ten diatom species from the Barents Sea at different irradiances and day lengths. *Marine Ecology Progress Series 64*, 169–173.

Grasshoff H. 1976. *Methods of sea water analysis*. Basel: Verlag Chemie.

Jones E.P. & Anderson L.G. 1986. On the origin of the chemical properties of the Arctic Ocean halocline. *Journal of Geophysical Research—Oceans 91*, 10759–10767.

Jones E.P., Anderson L.G. & Swift J.H. 1998. Distribution of Atlantic and Pacific waters in the upper Arctic Ocean: implications for circulation. *Geophysical Research Letters 25*, 765–768.

Junge K., Eicken H. & Deming J.W. 2004. Bacterial activity at −2 to −20°C in the Arctic wintertime sea ice. *Applied Environmental Microbiology 70*, 550–557.

Kinney P., Arhelger M.E. & Burrell D.C. 1970. Chemical characteristics of water masses in the Amerasian Basin of the Arctic Ocean. *Journal of Geophysical Research 75*, 4097–4104.

Kirkwood D.S. 1989. *Simultaneous determination of selected nutrients in sea water. Report CM 1989/C:29*. Copenhagen: International Council for the Exploration of the Seas.

Knap A.H., Michaels A., Close A.R., Ducklow H. & Dickson A.G. (eds.) 1996. *Protocols for the Joint Global Ocean Flux Study (JGOFS) core measurements. JGOFS Report 19*. Bremerhaven: Alfred Wegener Institute.

Krishfield R., Toole J., Proshutinsky A. & Timmermans M.-L. 2008. Automated ice-tethered profilers for seawater observations under pack ice in all seasons. *Journal of Atmospheric and Oceanic Technology 25*, 2091–2095.

Lansard B., Mucci A., Miller L.A., Macdonald R.W. & Gratton Y. 2012. Seasonal variability of water mass distribution in the southeastern Beaufort Sea determined by total alkalinity and $\delta^{18}O$. *Journal of Geophysical Research—Oceans 117*, C03003, doi: http://dx.doi.org/10.1029/2011JC007299

Lee S., Whiteledge T.E. & Kang S.-H. 2008. Carbon uptake rates of sea ice algae and phytoplankton under different light intensities in a landfast sea ice zone, Barrow, Alaska. *Arctic 61*, 281–291.

Lovejoy C., Vincent W.F., Bonilla S., Roy S., Martineau M.-J., Terrado R., Potvin M., Massana R. & Pedrós-Alió C. 2007. Distribution, phylogeny, and growth of cold-adapted picoprasinophytes in Arctic seas. *Journal of Phycology 43*, 78–89.

Macdonald R.W., Paton D.W., Carmack E.C. & Omstedt A. 1995. The freshwater budget and under-ice spreading of Mackenzie River water in the Canadian Beaufort Sea based on salinity and $^{18}O/^{16}O$ measurements in water and ice. *Journal of Geophysical Research—Oceans 100*, 895–919.

Mantoura R.F.C. & Woodward E.M.S. 1983. Optimization of the indophenol blue method for the automated determination of ammonia in estuarine waters. *Estuarine Coastal and Shelf Science 17*, 219–224.

Massman W.J. 1991. The attenuation of concentration fluctuations in turbulent flow through a tube. *Journal of Geophysical Research—Atmospheres 96*, 15269–15273.

Mathis J.T., Pickart R.S., Byrne R.H., McNeil C.L., Moore G.W.K., Juranek L.W., Liu X., Ma J., Easley R.A., Elliot M.M., Cross J.N., Reisdorph S.C., Bahr F., Morison J., Lichendorf T. & Feely R.A. 2012. Storm-induced upwelling of high pCO_2 waters onto the continental shelf of the western Arctic Ocean and implications for carbonate mineral saturation states. *Geophysical Research Letters 39*, L07606, doi: http://dx.doi.org/10.1029/2012GL051574

Mathis J.T., Pickart R.S., Hansell D.A., Kadko D. & Bates N.R. 2007. Eddy transport of organic carbon and nutrients from the Chukchi Shelf: impact on the upper halocline of the western Arctic Ocean. *Journal of Geophysical Research—Oceans 112*, C05011, doi: http://dx.doi.org/10.1029/2006JC003899

Mehrbach C., Culberson C.H., Hawley J.E. & Pytkowicz R.M. 1973. Measurements of the apparent dissociation constants of carbonic acid in seawater at atmospheric pressure. *Limnology and Oceanography 18*, 897–907.

Miller L.A., Chierici M., Johannessen T., Noji T.T., Rey F. & Skjelvan I. 1999. Seasonal dissolved inorganic carbon variations in the Greenland Sea and implications for atmospheric CO_2 exchange. *Deep-Sea Research Part II 46*, 1473–1496.

Miller L.A., Papakyriakou T.N., Collins R.E., Deming J.W., Ehn J.K., Macdonald R.W., Mucci A., Owens O., Raudsepp M. & Sutherland N. 2011. Carbon dynamics in sea ice: a winter flux time series. *Journal of Geophysical Research—Oceans 116*, C02028, doi: http://dx.doi.org/10.1029/2009JC006058

Miller L.A., Yager P.L., Erickson K.A., Amiel D., Bâcle J., Cochran J.K., Garneau M.-È., Gosselin M., Hirschberg D.J., Klein B., LeBlanc B. & Miller W.L. 2002. Carbon distributions and fluxes in the North Water, 1998 and 1999. *Deep-Sea Research Part II 49*, 5151–5170.

Moore C.J. 1986. Frequency response corrections for eddy correlation systems. *Boundary-Layer Meteorology 37*, 17–35.

Moore R.M., Lowings M.G. & Tan F.C. 1983. Geochemical profiles in the central Arctic Ocean: their relation to freezing and shallow circulation. *Journal of Geophysical Research—Oceans 88*, 2667–2674.

Mundy C.J., Gosselin M., Ehn J., Gratton Y., Rossnagel A., Barber D.G., Martin J., Tremblay J.-É., Palmer M., Arrigo K.R., Darnis G., Fortier L., Else B. & Papakyriakou T. 2009. Contribution of under-ice primary production to an ice-edge upwelling phytoplankton bloom in the Canadian Beaufort Sea. *Geophysical Research Letters 36*, L17601, doi: http://dx.doi.org/10.1029/2009GL038837

Mundy C.J., Gosselin M., Gratton Y., Brown K., Galindo V., Campbell K., Levasseur M., Barber D., Papakyriakou T. & Bélanger S. 2014. Role of environmental factors on phytoplankton bloom initiation under landfast sea ice in Resolute Passage, Canada. *Marine Ecology Progress Series 487*, 39–49.

Nguyen A.T., Menemenlis D. & Kwok R. 2011. Arctic ice–ocean simulation with optimized model parameters: approach and assessment. *Journal of Geophysical Research—Oceans 116*, C04025, doi: http://dx.doi.org/10.1029/2010JC006573

Olafsson J., Olafsdottir S.R., Benoit-Cattin A., Danielsen M., Arnarson T.S. & Takahashi T. 2009. Rate of Iceland Sea acidification from time series measurements. *Biogeosciences 6*, 2661–2668.

Orr J.C., Jutterström S., Bopp L., Anderson L.G., Bates N.R., Cadule P., Fabry V.J., Frölicker T., Heinze C., Jones E.P., Joos F., Key R.M., Lenton A., Maier-Reimer E., Olsen A., Segschneider J., Skjelvan I., Steinacher M., Swingedouw D. & Tjiptura J. 2010. Winter versus summer onset of undersaturation in the Arctic Ocean. Paper presented at the International Polar Year Oslo Science Conference. 8–12 June 2010, Oslo, Norway.

Orr J.C., Jutterström S., Bopp L., Anderson L.G., Cadule P., Fabry V.J., Frölicher T., Jones E.P., Joos F., Lenton A., Maier-Reimer E., Segschneider J., Steinacher M. & Swingedouw D. 2009. Amplified acidification in the Arctic ocean. *IOP Conference Series Earth and Environmental Science 6*, article no. 462009, doi: http://dx.doi.org/10.1088/1755-1307/6/6/462009

Papakyriakou T. & Miller L. 2011. Springtime CO_2 exchange over seasonal sea ice in the Canadian Arctic Archipelago. *Annuals of Glaciology 52*, 215–224.

Perovich D.K., Richter-Menge J.A., Jones K.F. & Light B. 2008. Sunlight, water and ice: extreme Arctic sea ice melt during summer of 2007. *Geophysical Research Letters 35*, L11501, doi: http://dx.doi.org/10.1029/2008GL034007

Pierrot D., Lewis E. & Wallace D.W.R. 2006. *MS Excel program developed for CO_2 system calculations. ORNL/CDIAC-105a*. Oak Ridge, TN: Carbon Dioxide Information Analysis Center, Oak Ridge National Laboratory, US Department of Energy.

Popova E.E., Yool A., Aksenov Y., Coward A.C. & Anderson T.R. 2014. Regional variability of acidification in the Arctic: a sea of contrasts. *Biogeosciences 11*, 293–308.

Popova E.E., Yool A., Coward A.C., Aksenov Y.K., Alderson S.G., de Cuevas B.A. & Anderson T.R. 2010. Control of primary production in the Arctic by nutrients and light: insights from a high resolution ocean general circulation model. *Biogeosciences 7*, 3569–359.

Prinsenberg S.J. & Ingram R.G. 1991. Under-ice physical oceanography processes. *Journal of Marine Systems 2*, 143–152.

Proshutinsky A.Y. & Johnson M. 2001. Two regimes of the Arctic's circulation from ocean models with ice and contaminants. *Marine Pollution Bulletin 43*, 61–70.

Rysgaard S., Glud R.N., Sejr M.K., Bendtsen J. & Christensen P.B. 2007. Inorganic carbon transport during sea ice growth and decay: a carbon pump in polar seas. *Journal of Geophysical Research—Oceans 112*, C03016, doi: http://dx.doi.org/10.1029/2006JC003572

Semiletov I., Makshtas A., Akasofu S.-I. & Andreas E.L. 2004. Atmospheric CO_2 balance: the role of Arctic sea ice. *Geophysical Research Letters 31*, L05121, doi: http://dx.doi.org/10.1029/2003GL017996

Shadwick E.H., Thomas H., Chierici M., Else B., Fransson A., Michel C., Miller L.A., Mucci A., Niemi A., Papakyriakou T.N. & Tremblay J.-É. 2011. Seasonal variability of the inorganic carbon system in the Amundsen Gulf region of the southeastern Beaufort Sea. *Limnology and Oceanography 56*, 303–322.

Shadwick E.H., Trull T.W., Thomas H. & Gibson J.A.E. 2013. Vulnerability of polar oceans to anthropogenic acidification: comparison of Arctic and Antarctic seasonal cycles. *Scientific Reports 3*, 2339–2346.

Skjelvan I., Falck E., Rey F. & Kringstad S.B. 2008. Inorganic carbon time series at Ocean Weather Station M in the Norwegian Sea. *Biogeosciences 5*, 549–560.

Stein R. & Macdonald R.W. (eds.) 2004. *The organic carbon cycle in the Arctic Ocean*. Berlin: Springer.

Tanner C.B. & Thurtell G.W. 1969. *Anemoclinometer measurements of reynolds stress and heat transport in the atmospheric surface layer. Research and Development Technical Report ECOM 66-G22-F to the US Army Electronics Command*. Madison: Department of Soil Science, University of Wisconsin.

Tremblay J.-É., Simpson K., Martin J., Miller L., Gratton Y., Barber D. & Price N.M 2008. Vertical stability and the annual dynamics of nutrients and chlorophyll fluorescence in the coastal, southeast Beaufort Sea. *Geophysical Research Letters 113*, C07S90, doi: http://dx.doi.org/10.1029/2007JC004547

Toole J.M., Timmermans M.-L., Perovich D.K., Krishfield R.A., Proshutinsky A. & Richter-Menge J.A. 2010. Influences of the ocean surface mixed layer and thermohaline stratification on Arctic Sea ice in the central Canada Basin. *Journal of Geophysical Research—Oceans 115*, C10018, doi: http://dx.doi.org/10.1029/2009JC005660

Williams W.J., Carmack E.C., Shimada K., Melling H., Aagaard K., Macdonald R.W. & Ingram R.G. 2006. Joint effects of wind and ice motion in forcing upwelling in Mackenzie Trough, Beaufort Sea. *Continental Shelf Research 26*, 2352–2366.

Woodward E.M.S. & Rees A.P. 2001. Nutrient distributions in an anticyclonic eddy in the northeast Atlantic Ocean, with reference to nanomolar ammonium concentrations. *Deep-Sea Research Part II 48*, 775–793.

Zemmelink H.J., Delille B., Tison J.L., Hinsta E.J., Houghton L. & Dacey J.W.H. 2006. CO_2 deposition over the multi-year ice of the western Weddell Sea. *Geophysical Research Letters 33*, L13606, doi: http://dx.doi.org/10.1029/2006GL026320

Zhang J.-Z. & Chi J. 2002. Automated analysis of nanomolar concentrations of phosphate in natural waters with liquid waveguide. *Environmental Science and Technology 36*, 1048–1053.